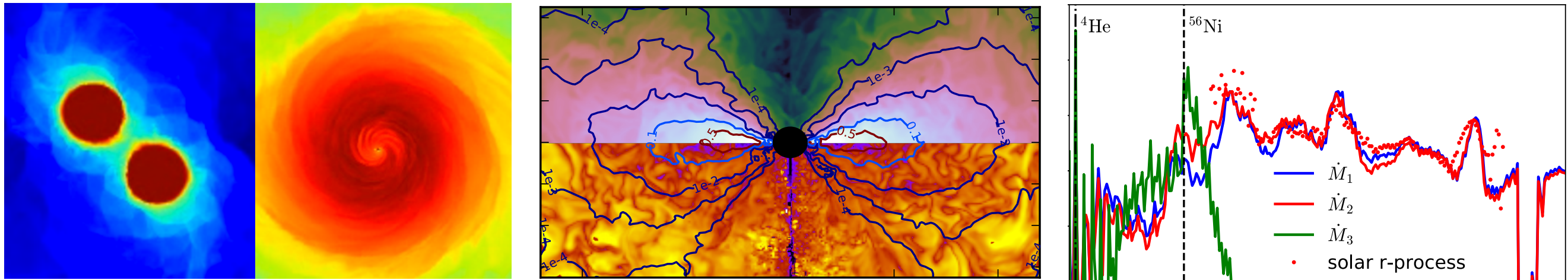


ICTP school: kilonovae slides



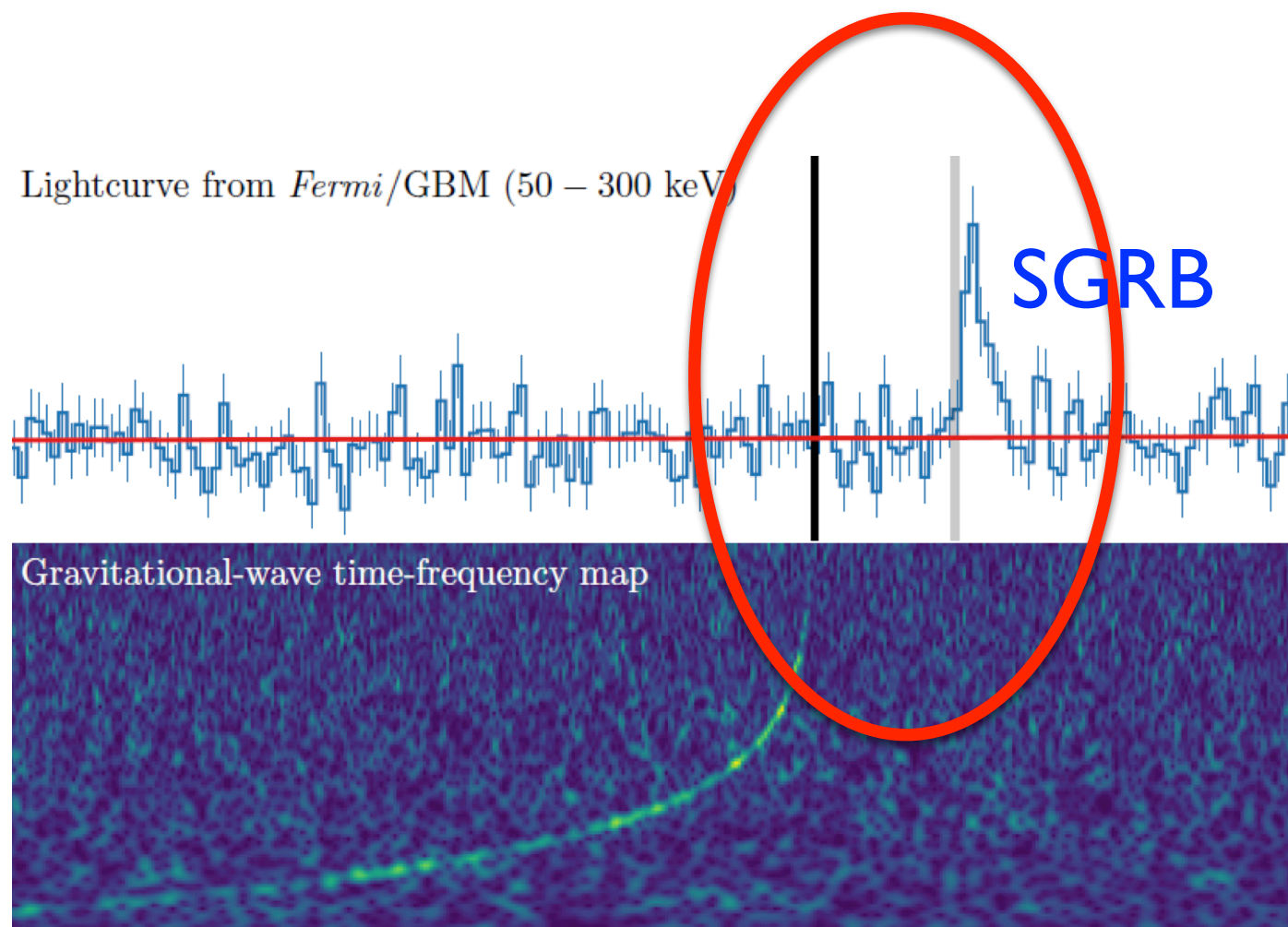
Daniel M. Siegel

Center for Theoretical Physics & Columbia Astrophysics Laboratory

Columbia University

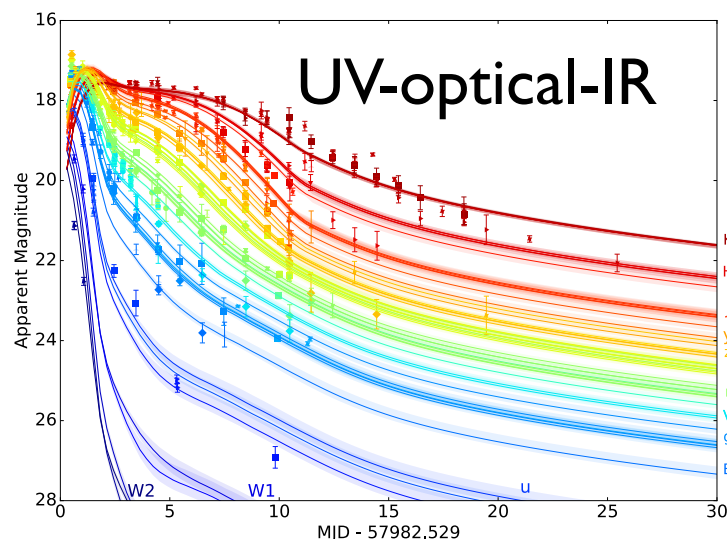
ICTP school *The Sound of Space-time: The Dawn of Gravitational Wave Science*,
Sao Paulo, Dec 10-14, 2018

GW170817 and the fireworks of EM counterparts

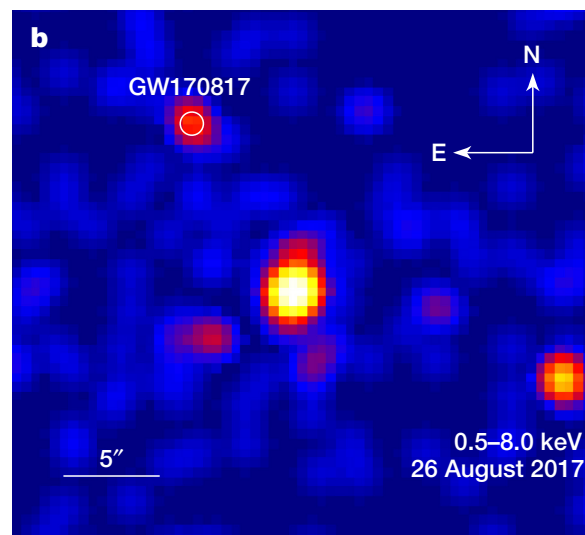


- **unique event in astronomy**, maybe most important observation since SN 1987A
- unprecedented level of multi-messenger observations
- confirms **association of BNS to SGRBs**
- **kilonova** provides strong evidence for synthesis of **r-process material**

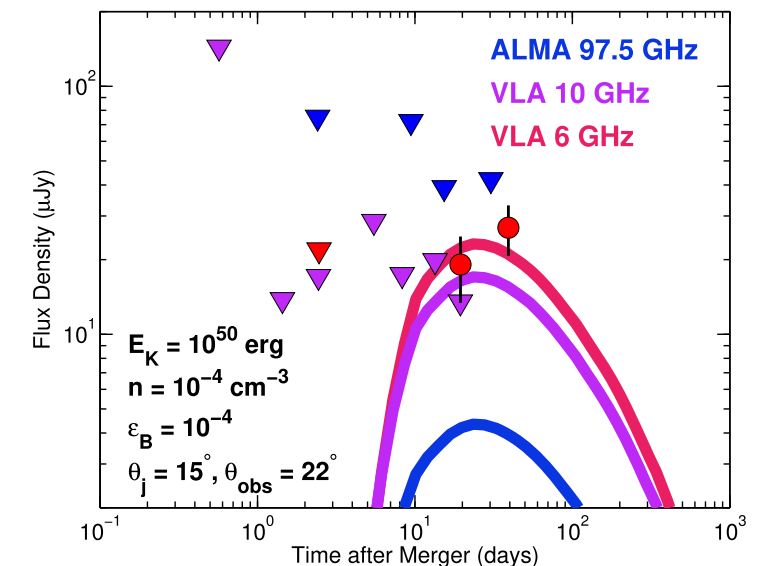
kilonova



X-rays



radio



The kilonova of GW170817

- **blue** kilonova properties:

$$M_{\text{ej}} \sim 10^{-2} M_{\text{sun}} \quad \text{Kilpatrick+ 2017}$$

$$v_{\text{ej}} \sim 0.2-0.3c \quad \text{Kasen+ 2017}$$

$$Y_e > 0.25 \quad \text{Nicholl+ 2017}$$

$$X_{\text{La}} < 10^{-4} \quad \text{Villar+ 2017}$$

‘lanthanide-free’

- **red** kilonova properties:

$$M_{\text{ej}} \sim 4-5 \times 10^{-2} M_{\text{sun}} \quad \text{Kilpatrick+ 2017}$$

$$v_{\text{ej}} \sim 0.08-0.14c \quad \text{Kasen+ 2017}$$

$$Y_e < 0.25 \quad \text{Kasliwal+ 2017}$$

$$X_{\text{La}} \sim 0.01 \quad \text{Drout+ 2017}$$

$$\quad \text{Cowperthwaite+ 2017}$$

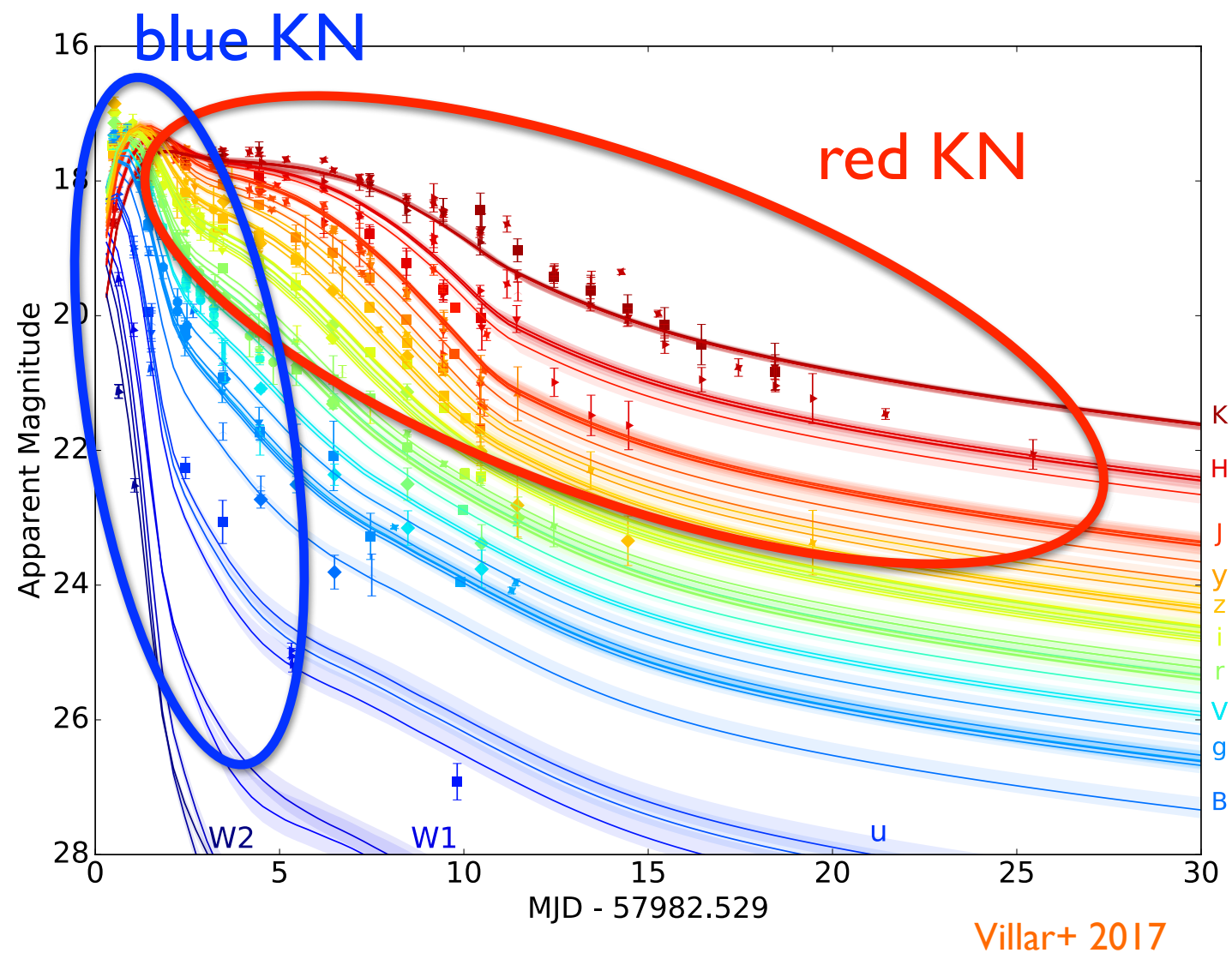
$$\quad \text{Chornock+ 2017}$$

$$\quad \text{Villar+ 2017}$$

$$\quad \text{Coughlin+ 2018}$$

heavy r-process elements!

‘lanthanide-rich’

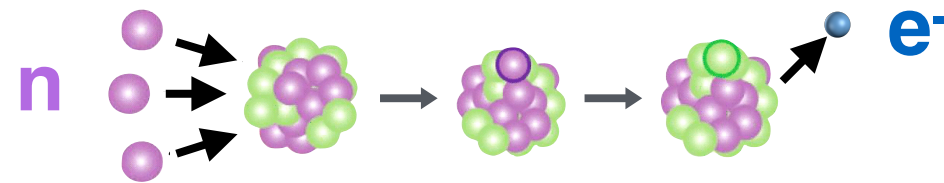


two (“red-blue”) or multiple components **expected from merger simulations**
(we shall see later)

The r-process in a nutshell

The r-process and s-process

The heavy elements ($A > 62$) are formed by neutron capture onto seed nuclei

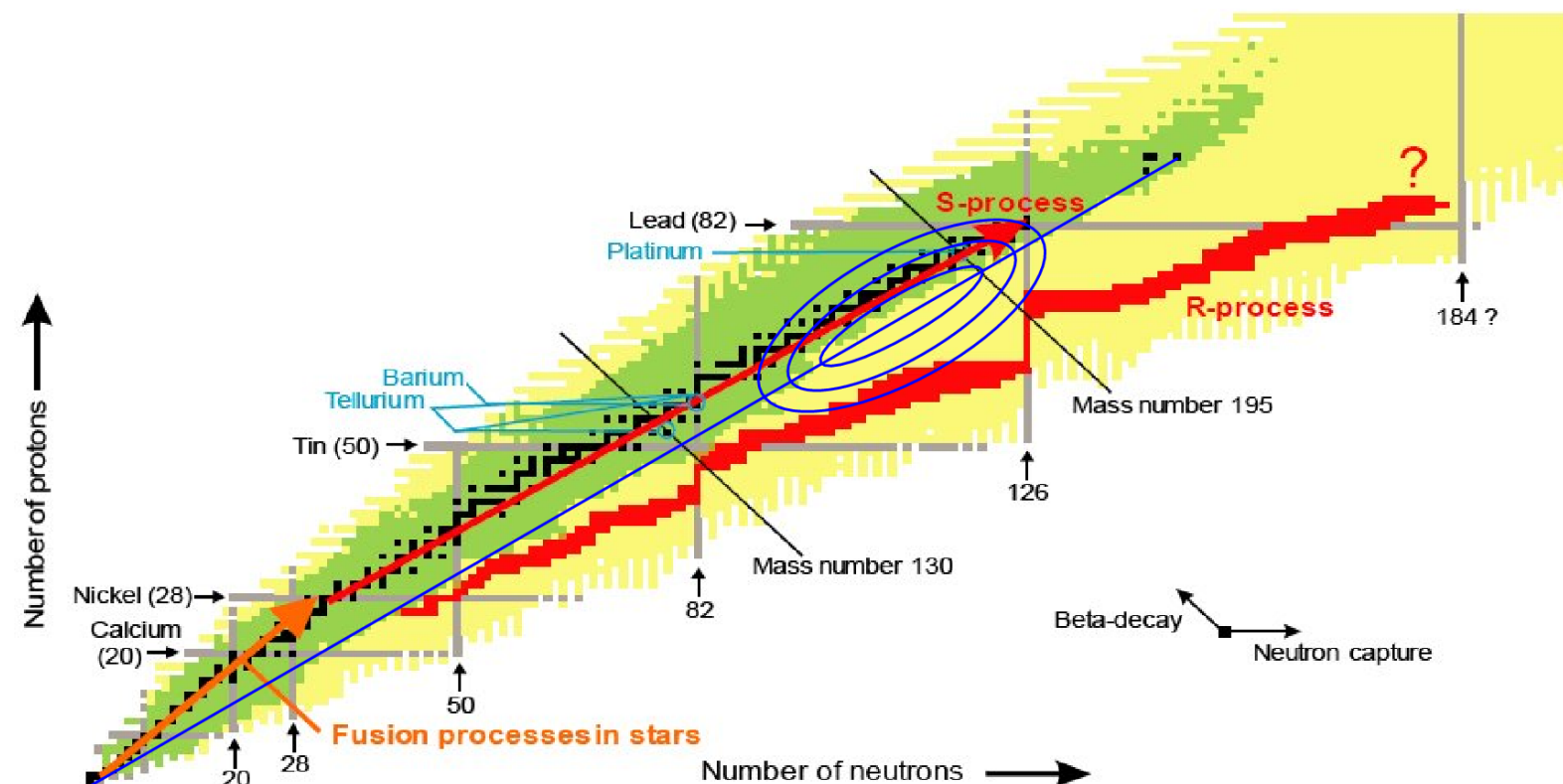


slow neutron capture (s-process):

timescale for neutron capture longer than for β -decay

rapid neutron capture (r-process):

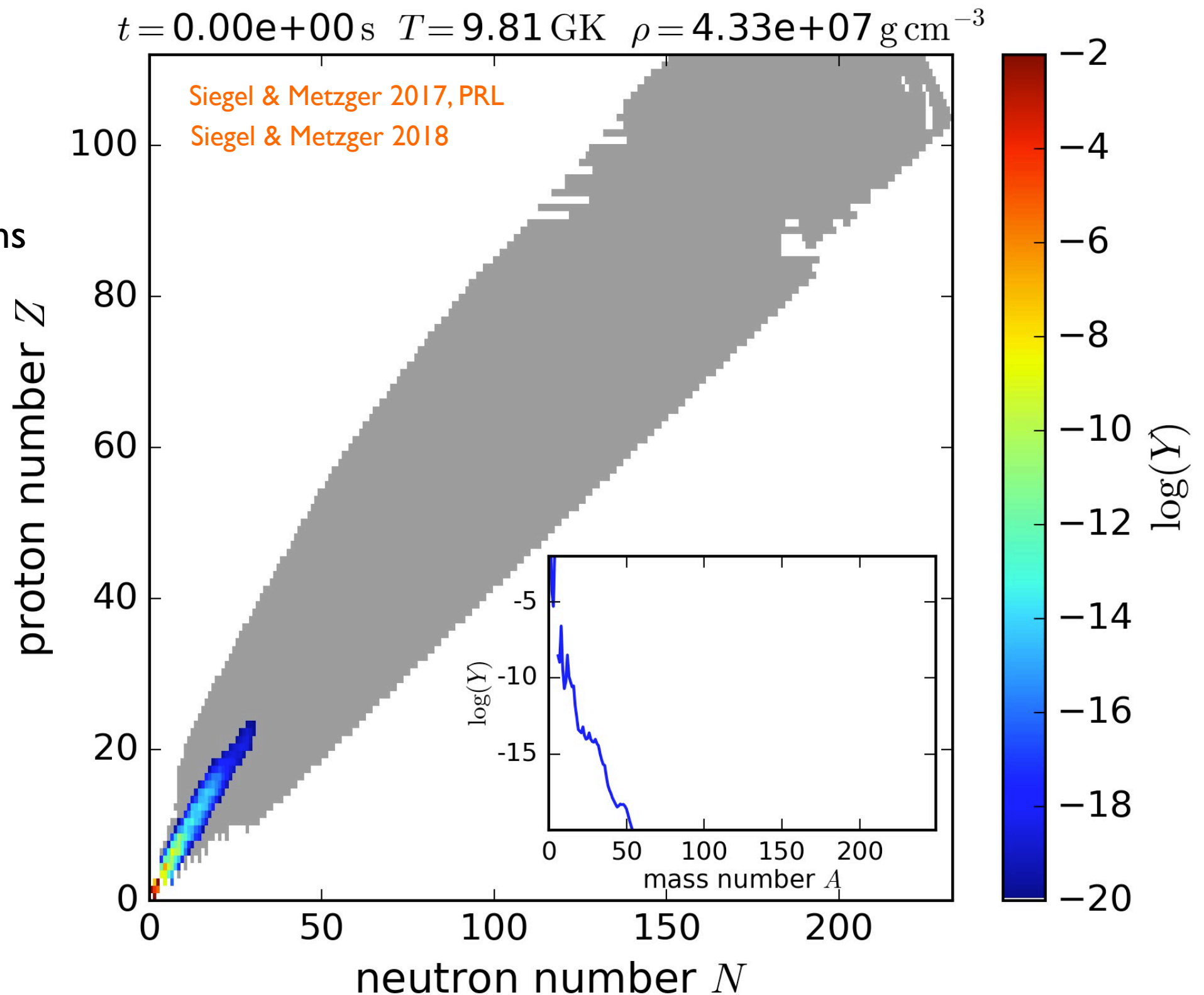
timescale for neutron capture shorter than for β -decay



r-process nucleosynthesis in disk outflows

nuclear reaction
network
(SkyNet)

- neutron captures
- photo-dissociations
- α -, β -decays
- fission



Movie: r-process nucleosynthesis from NS merger remnant disks

Heating rates

Heating rates

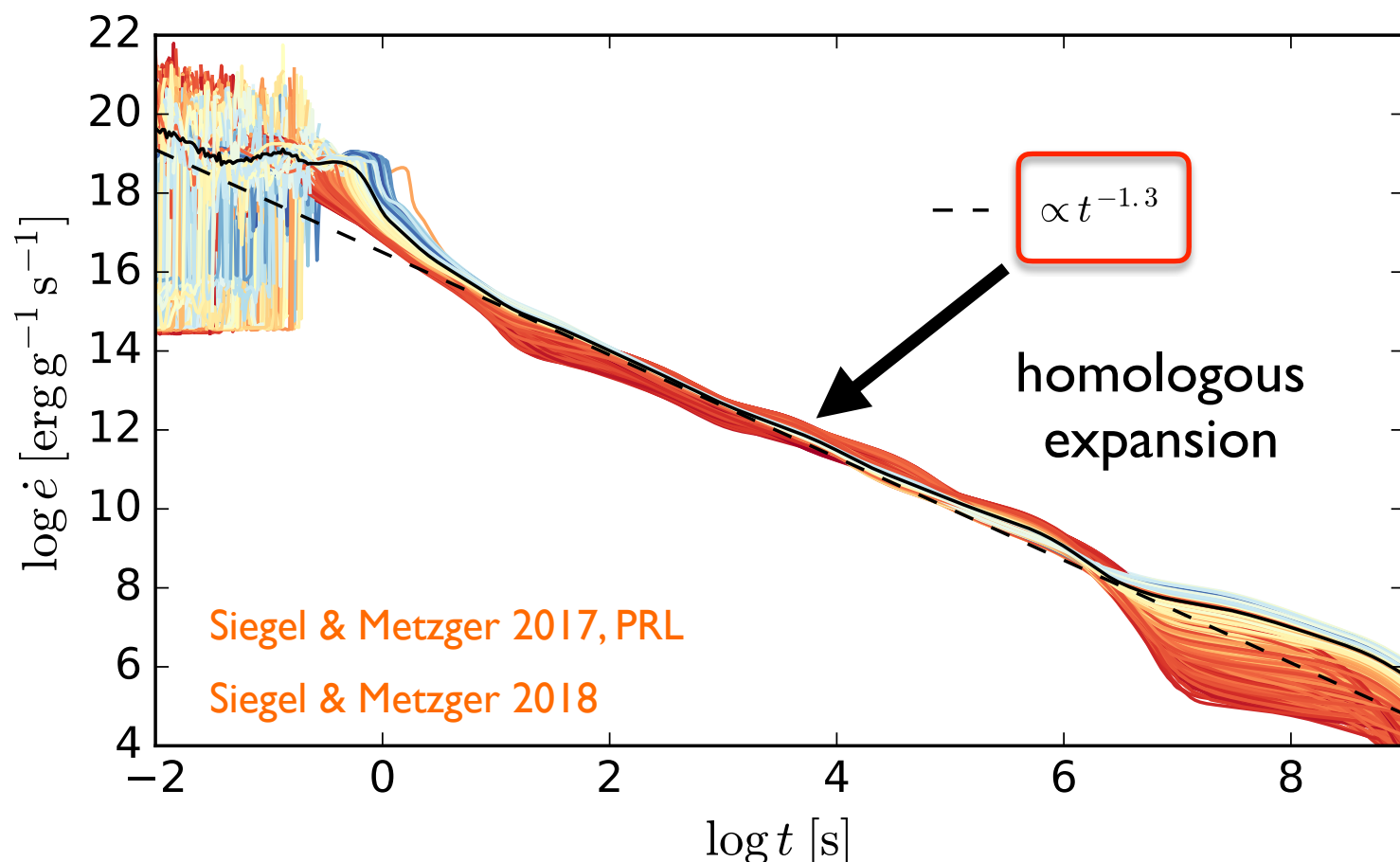
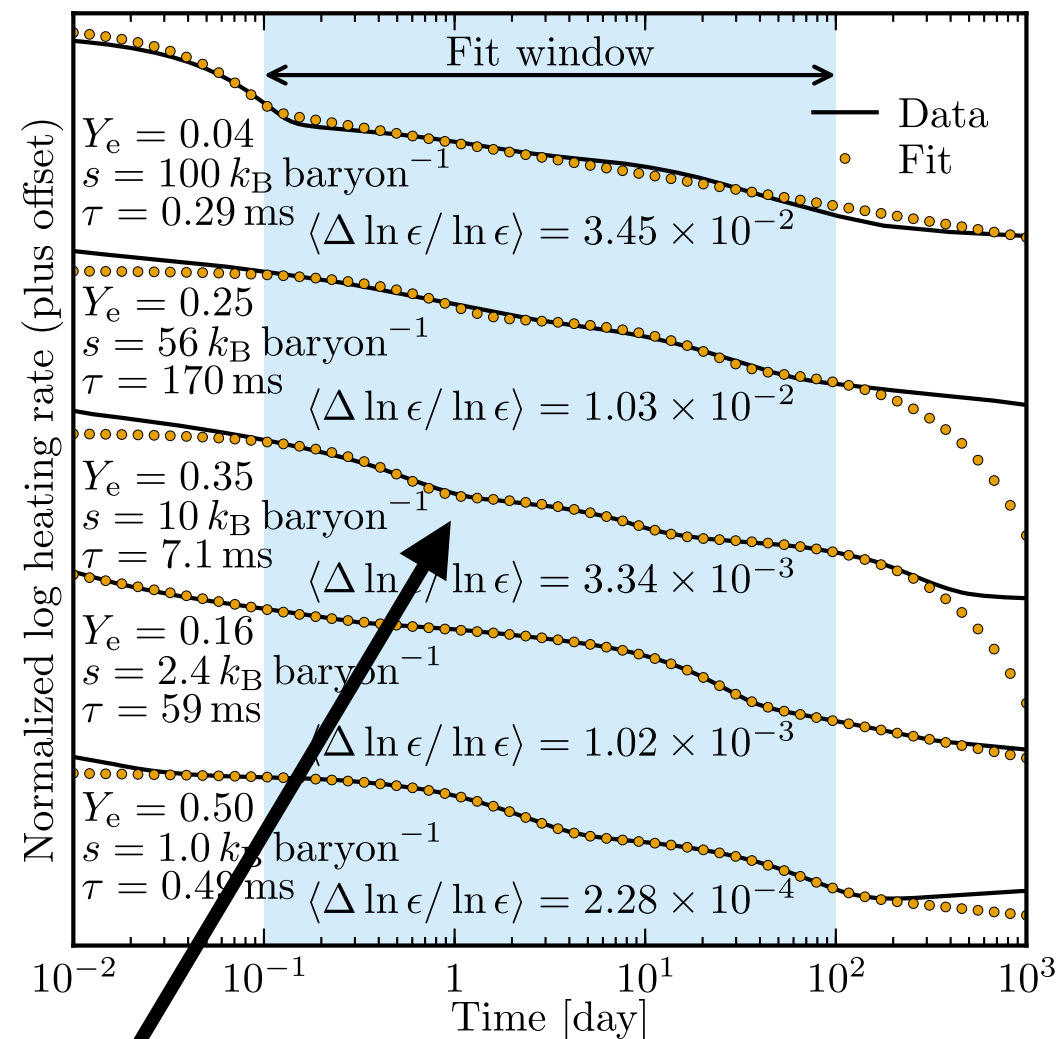


Fig: heating rates from r-process nucleosynthesis in simulations of post-merger disk outflows (lanthanide rich).

bumps and wiggles appear for lanthanide-poor conditions due to dominance of individual isotopes



Lippuner & Roberts 2015

Fig: heating rates from r-process nucleosynthesis for individual trajectories, varying electron fraction, specific entropy and the expansion timescale.

Bumps due to single isotopes expected even in lanthanide-rich scenario on timescales ~months
 → may lead to observational identification of specific isotopes Wu+ 2018

Thermalization efficiency

Barnes+ 2016

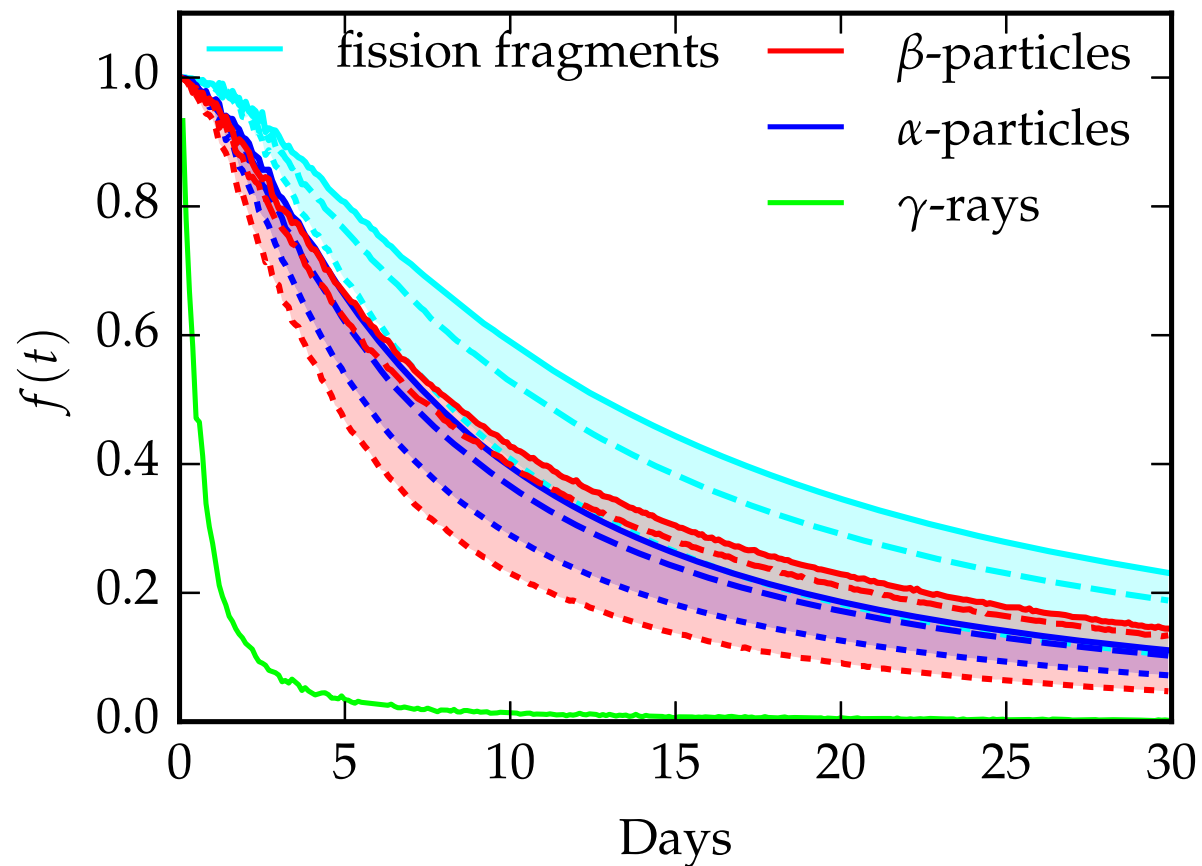


Fig: Example of thermalization efficiencies for all particles, assuming ejecta with $M_{\text{ej}} = 5e-3 M_{\text{sun}}$, $v_0 = 0.2c$.

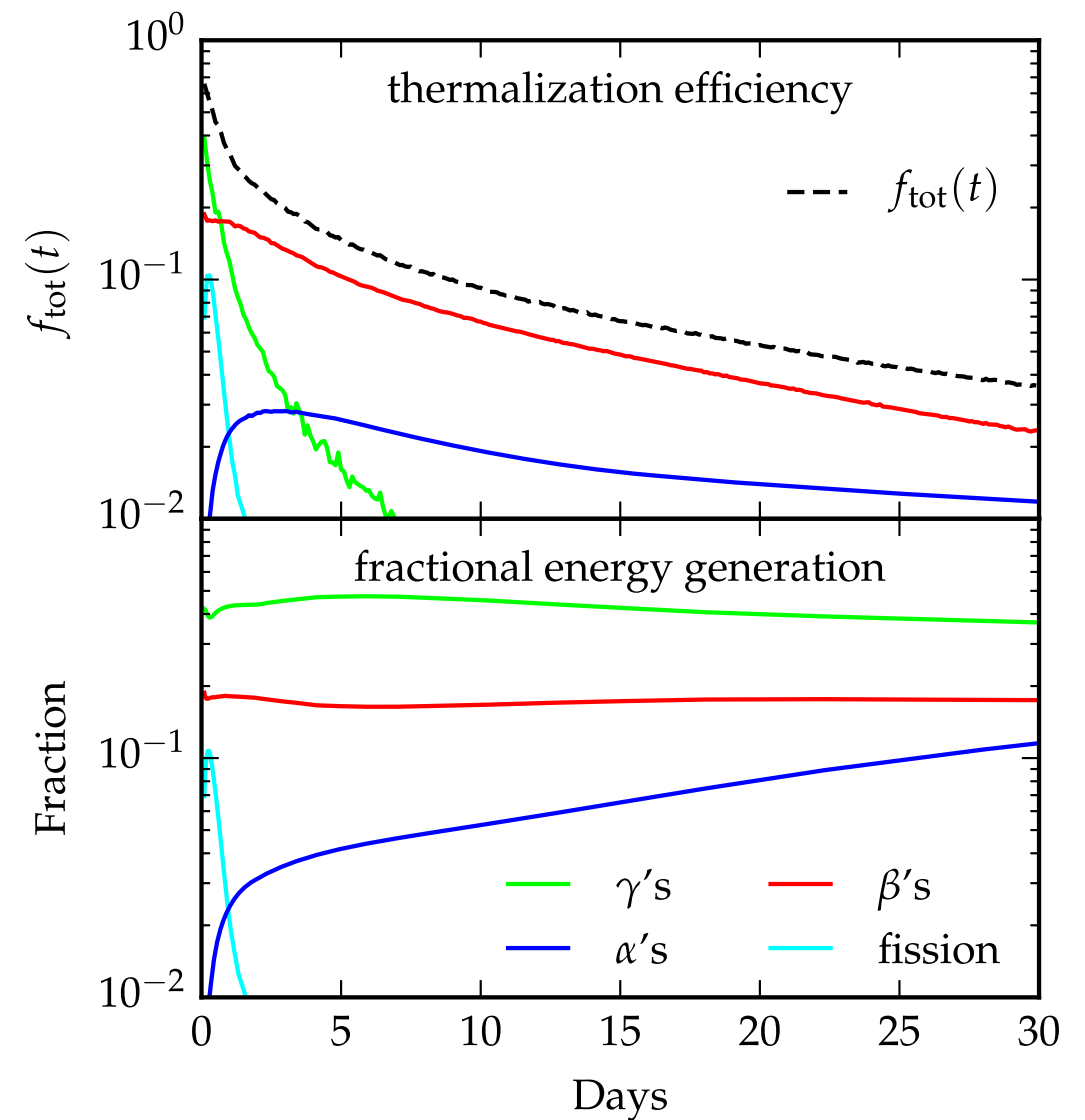


Fig: Thermalization efficiency of all particles convolved with their fractional energy generation.

Effect of thermalization efficiency on lightcurves

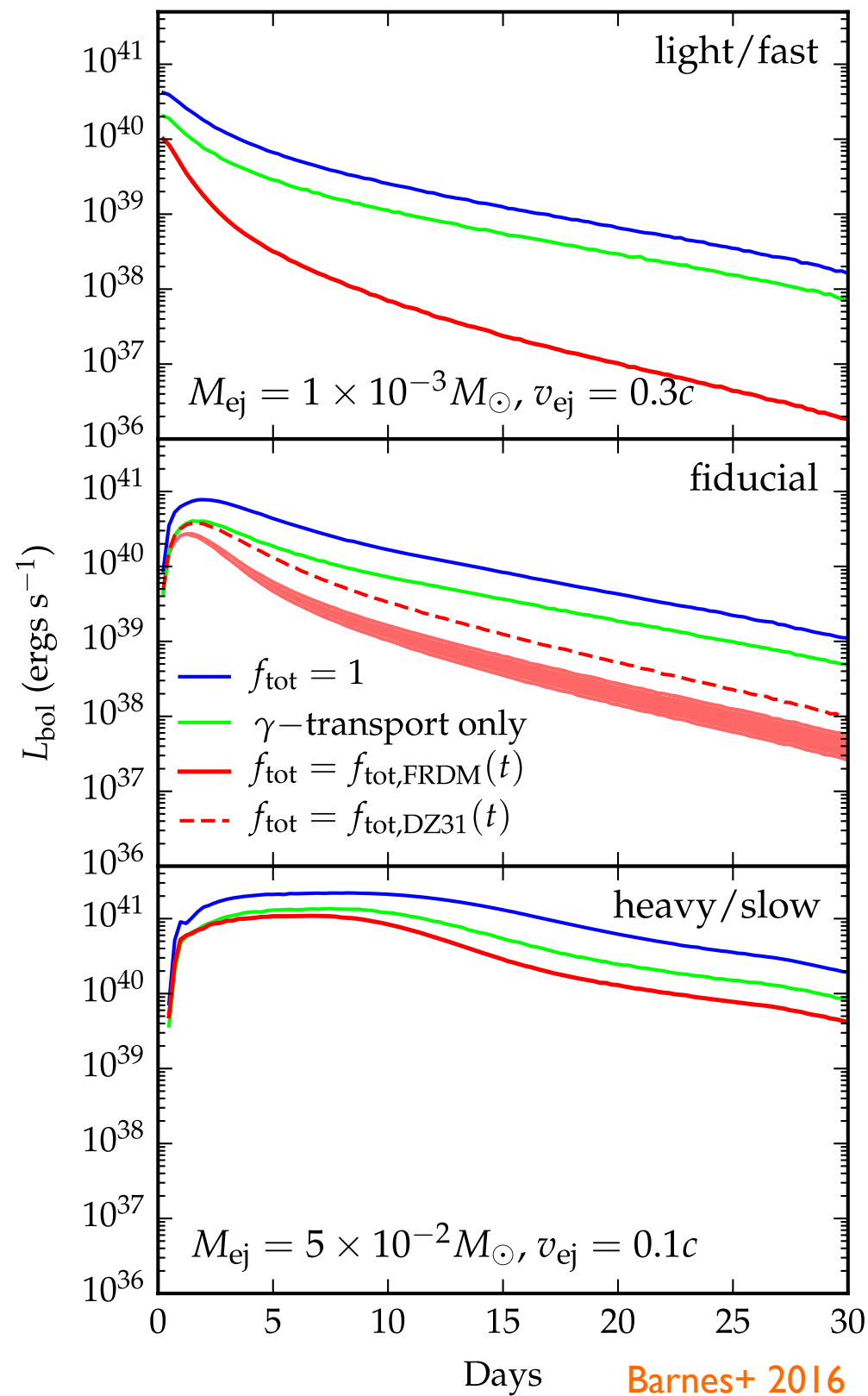
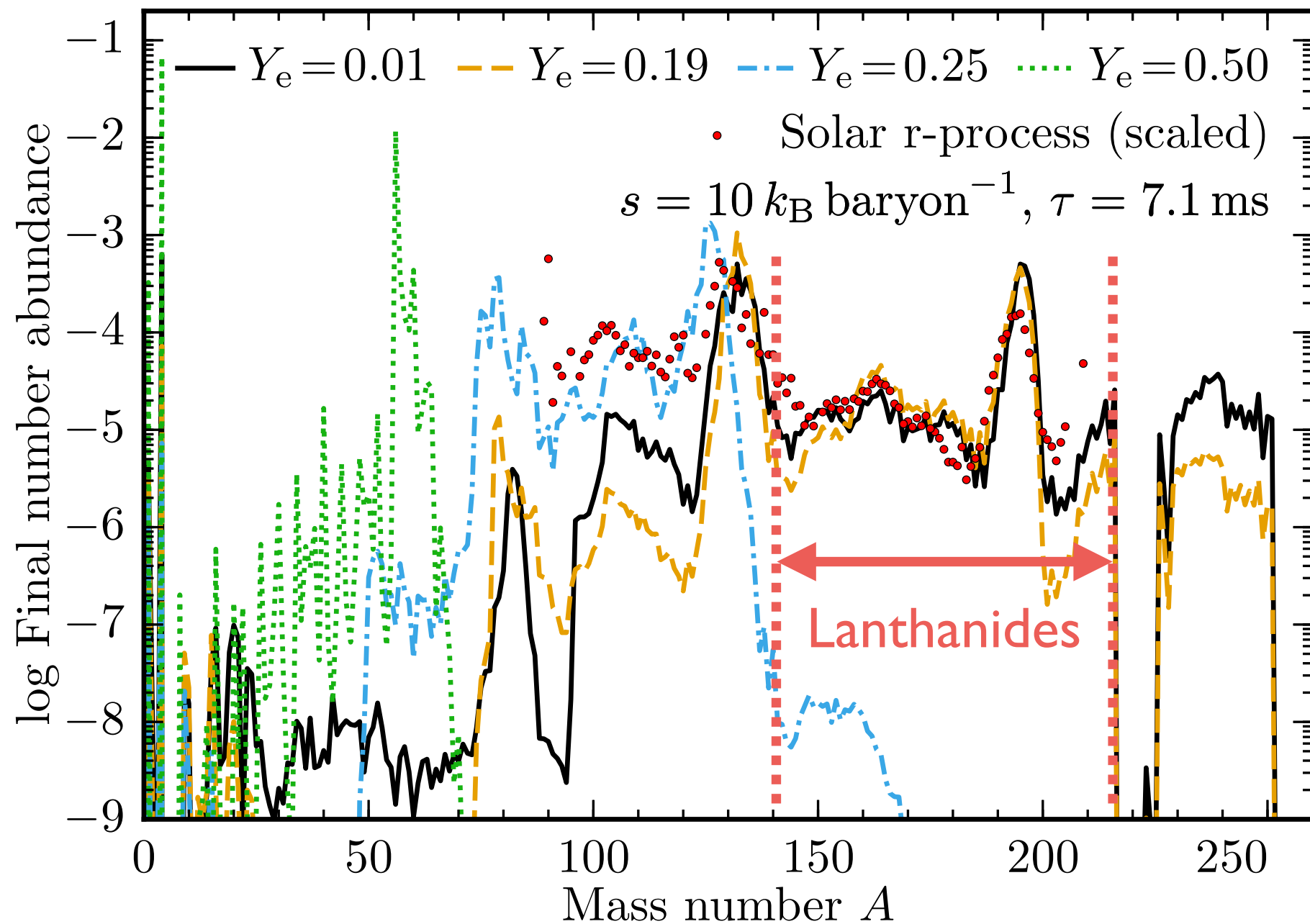


Fig: Impact of thermalization efficiency on kilonova lightcurves (bolometric luminosity). The fiducial model has parameters $M_{\text{ej}} = 5 \times 10^{-3} M_{\odot}$, $v_0 = 0.2c$.

Opacities

Outcome of the r-process

fewer free n per seed nucleus \longleftrightarrow more free n per seed nucleus



Lippuner & Roberts 2015

Final abundance pattern depends strongly on initial composition (Y_e)!

High opacities of the Lanthanides

Kasen+ 2013, Barnes & Kasen 2013

Number of electron configurations
for a shell with g levels and n electrons:

$$N_{\text{conf}} \sim \frac{g!}{n!(g-n)!}$$

s-shell ($g=2$)

p-shell ($g=6$)

d-shell ($g=10$)

1 H 1s																	2 He 1s						
3 Li 2s	4 Be																	5 B 2p	6 C	7 N	8 O	9 F	10 Ne
11 Na 3s	12 Mg																	13 Al 3p	14 Si	15 P	16 S	17 Cl	18 Ar
19 K 4s	20 Ca	21 Sc	22 Ti	23 V	24 Cr	25 Mn	26 Fe	27 Co	28 Ni	29 Cu	30 Zn	31 Ga	32 Ge	33 As	34 Se	35 Br	36 Kr	49 In	50 Sn	51 Sb	52 Te	53 I	54 Xe
37 Rb 5s	38 Sr	39 Y	40 Zr	41 Nb	42 Mo	43 Tc	44 Ru	45 Rh	46 Pd	47 Ag	48 Cd	49 In	50 Sn	51 Sb	52 Te	53 I	54 Xe	81 Tl	82 Pb	83 Bi	84 Po	85 At	86 Rn
55 Cs 6s	56 Ba	57 La	72 Hf	73 Ta	74 W	75 Re	76 Os	77 Ir	78 Pt	79 Au	80 Hg	81 Tl	82 Pb	83 Bi	84 Po	85 At	86 Rn	113	114				
87 Fr 7s	88 Ra	89 Ac	104 Rf	105 Db	106 Sg	107 Bh	108 Hs	109 Mt	110	111	112	113	114										
		58 Ce	59 Pr	60 Nd	61 Pm	62 Sm	63 Eu	64 Gd	65 Tb	66 Dy	67 Ho	68 Er	69 Tm	70 Yb	71 Lu								
		90 Th	91 Pa	92 U	93 Np	94 Pu	95 Am	96 Cm	97 Bk	98 Cf	99 Es	100 Fm	101 Md	102 No	103 Lr								

$$N_{\text{conf}} \sim \frac{g!}{n!(g-n)!}$$

d-shell (g=10)

p-shell (g=6)

f-shell (g=14)

f-shell ($g=14$)

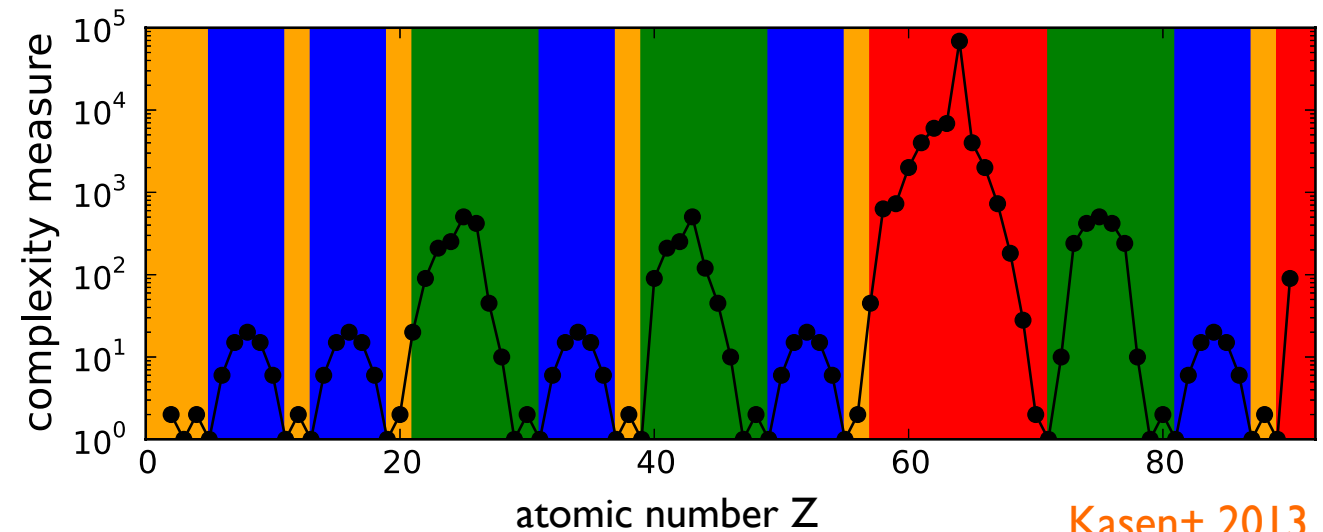
High opacities of the Lanthanides

Kasen+ 2013, Barnes & Kasen 2013

open shells

configurations: $N_{\text{conf}} = \prod_i \frac{g_i!}{n_i!(g_i - n_i)!}$

opacity: $\kappa \sim N_{\text{lines}} \sim N_{\text{conf}}^2$



s-shell (g=2)

1 H 1s																	2 He 1s						
3 Li 2s	4 Be																	5 B 2p	6 C	7 N 2p	8 O 2p	9 F 2p	10 Ne 2p
11 Na 3s	12 Mg																	13 Al 3p	14 Si 3p	15 P 3p	16 S 3p	17 Cl 3p	18 Ar 3p
19 K 4s	20 Ca	21 Sc	22 Ti	23 V	24 Cr	25 Mn 3d	26 Fe 3d	27 Co 3d	28 Ni 3d	29 Cu 3d	30 Zn 3d	31 Ga	32 Ge	33 As 4p	34 Se 4p	35 Br 4p	36 Kr 4p	49 In	50 Sn	51 Sb 5p	52 Te 5p	53 I 5p	54 Xe 5p
37 Rb 5s	38 Sr	39 Y	40 Zr	41 Nb	42 Mo	43 Tc 4d	44 Ru 4d	45 Rh 4d	46 Pd 4d	47 Ag 4d	48 Cd 4d	49 In	50 Sn	51 Sb 5p	52 Te 5p	53 I 5p	54 Xe 5p	81 Tl	82 Pb	83 Bi 6p	84 Po 6p	85 At 6p	86 Rn 6p
55 Cs 6s	56 Ba	57 La	72 Hf	73 Ta	74 W	75 Re 5d	76 Os 5d	77 Ir 5d	78 Pt 5d	79 Au 5d	80 Hg 5d	81 Tl	82 Pb	83 Bi 6p	84 Po 6p	85 At 6p	86 Rn 6p	113	114				
87 Fr 7s	88 Ra	89 Ac	104 Rf	105 Db	106 Sg	107 Bh 6d	108 Hs 6d	109 Mt	110	111	112	113	114										
		58 Ce	59 Pr	60 Nd	61 Pm	62 Sm	63 Eu	64 Gd 4f	65 Tb 4f	66 Dy	67 Ho	68 Er	69 Tm	70 Yb	71 Lu								
		90 Th	91 Pa	92 U	93 Np	94 Pu	95 Am	96 Cm 5f	97 Bk 5f	98 Cf	99 Es	100 Fm	101 Md	102 No	103 Lr								

f-shell (g=14)

shells: s p d f

High opacities of the Lanthanides

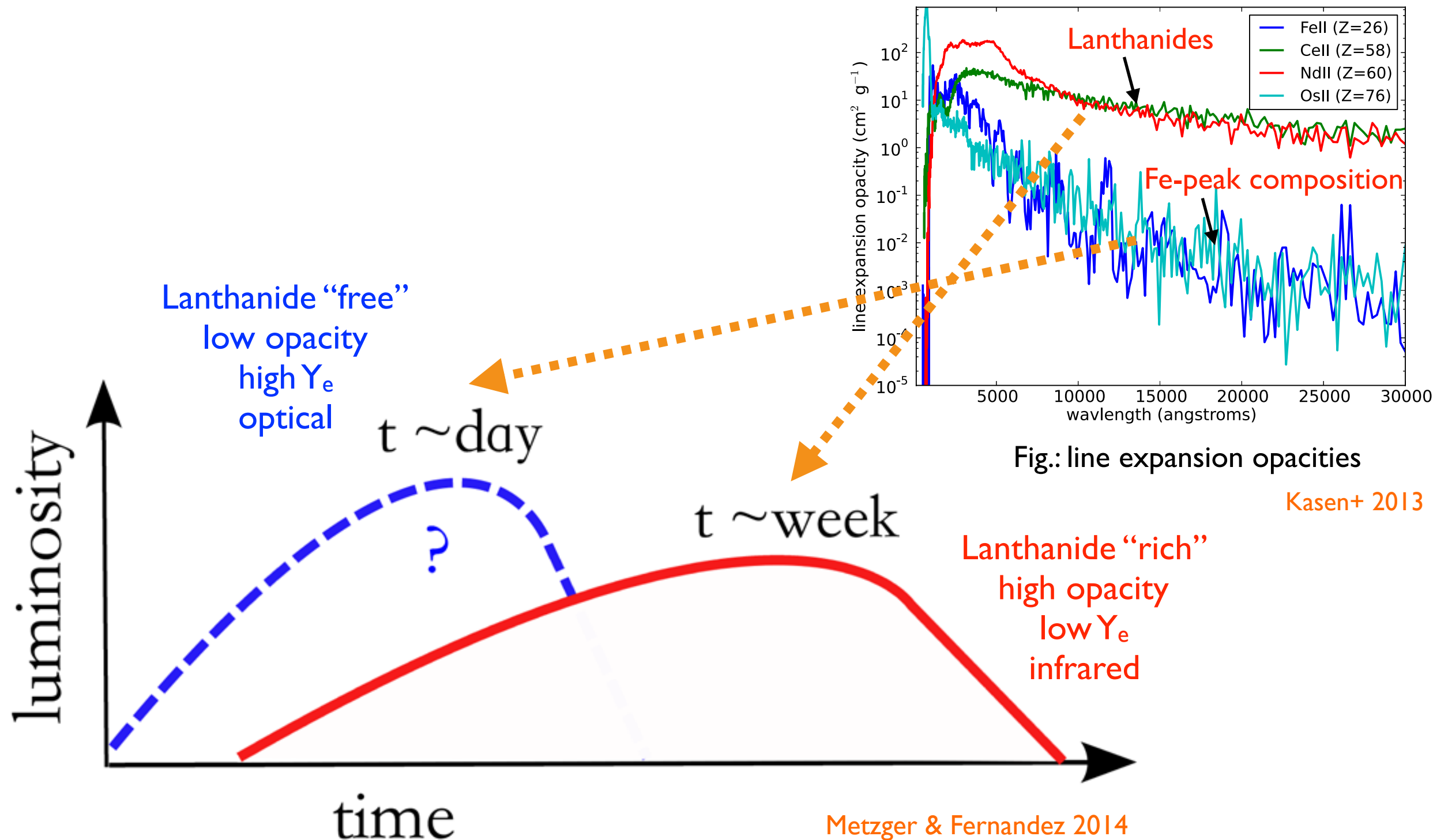
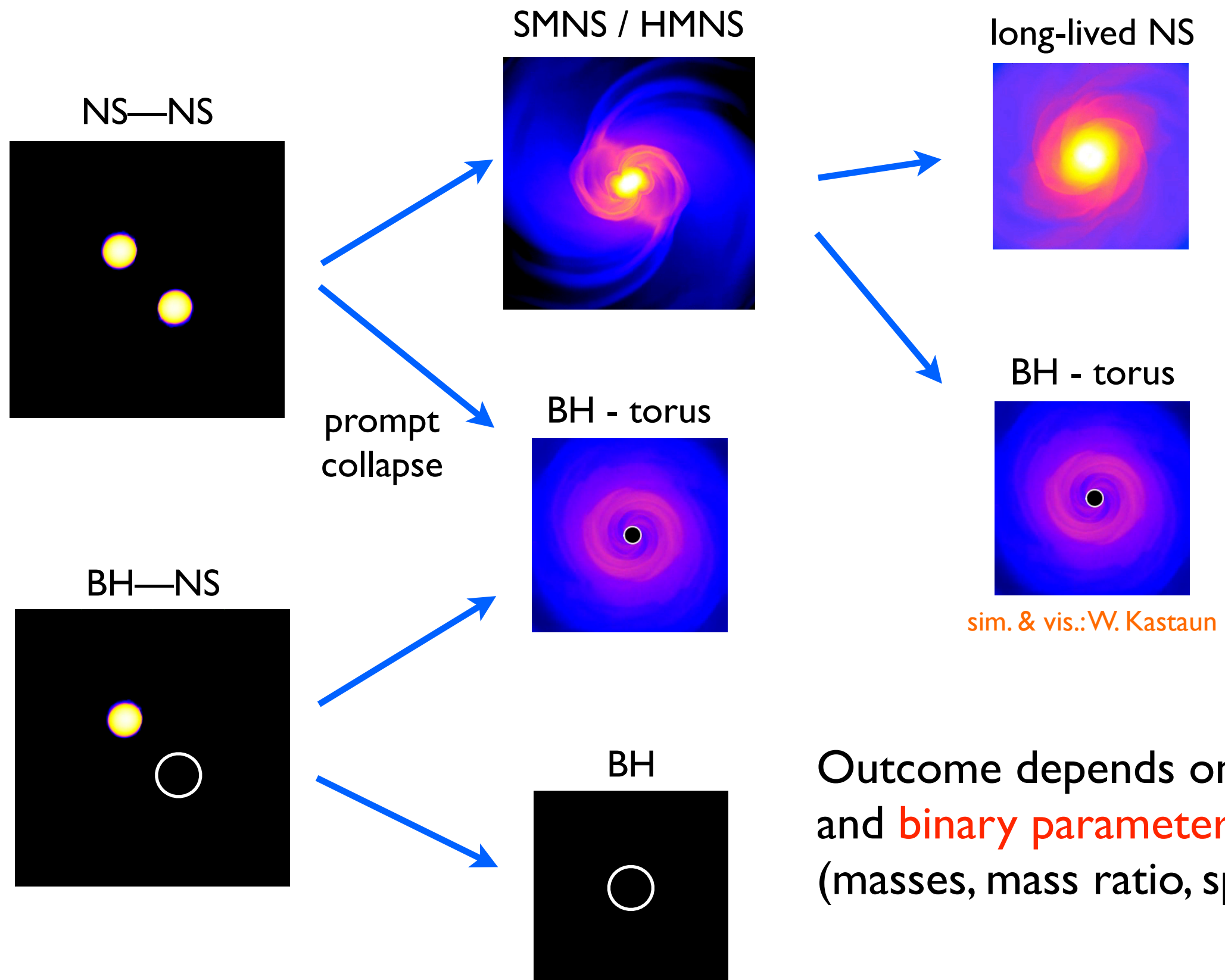


Fig.: kilonova lightcurves probe composition (Lanthanide mass fraction).

Origin of neutron-rich ejecta

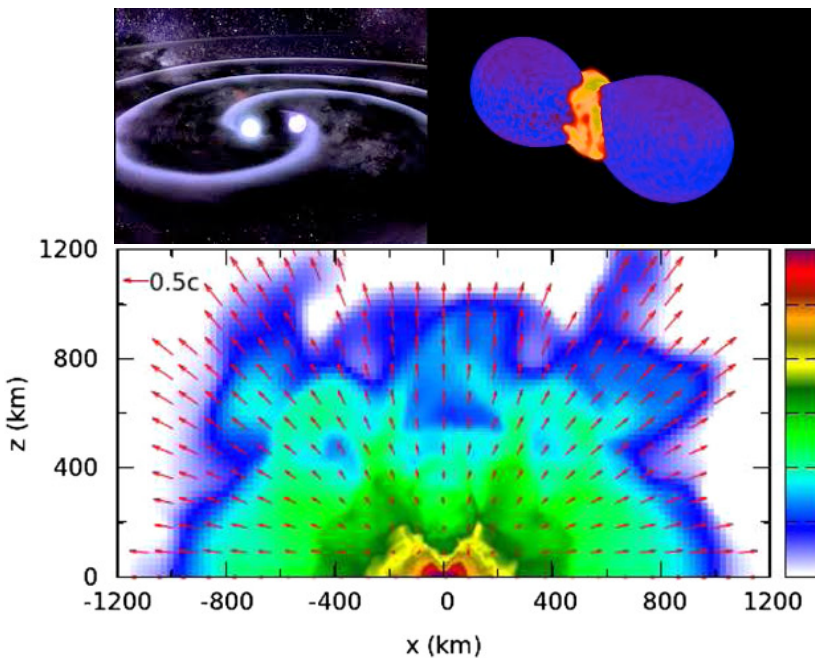
NS merger phenomenology



Outcome depends on **EOS**
and **binary parameters**
(masses, mass ratio, spin, ...)

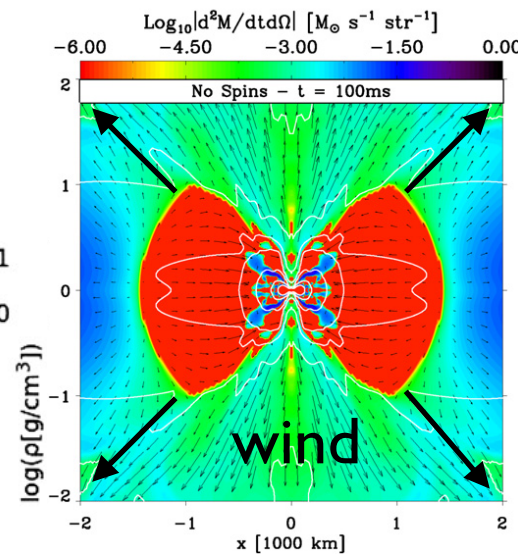
Sources of ejecta in NS mergers

dynamical ejecta (\sim ms)

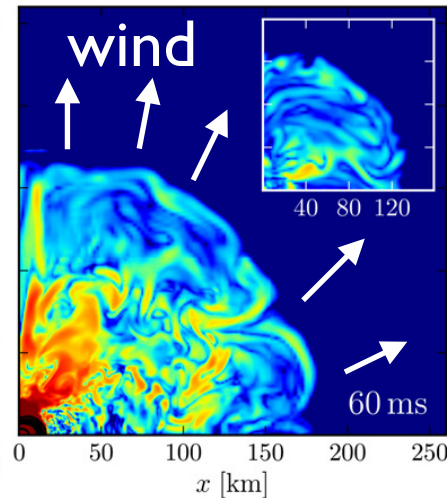


Hotokezaka+ 2013, Bauswein+ 2013

winds from NS remnant (\sim 10ms-1s)

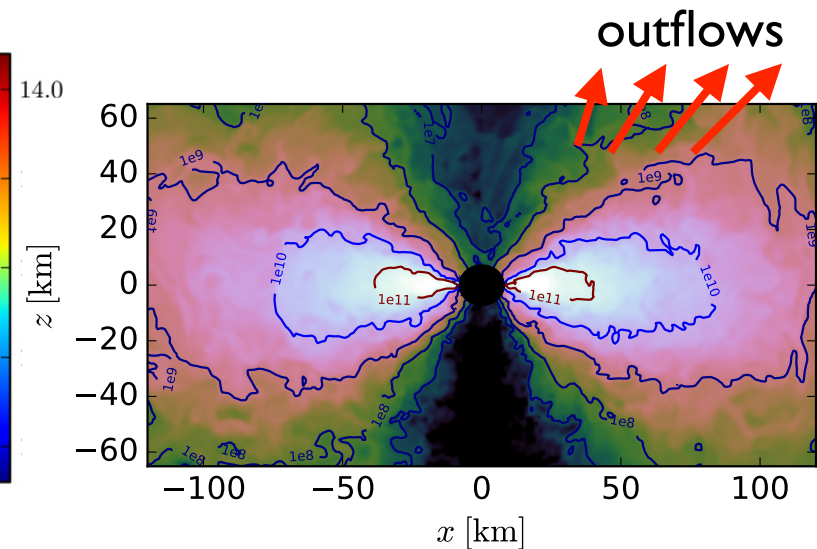


Dessart+ 2009



Siegel+ 2014
Ciolfi, Siegel+ 2017

accretion disk (\sim 10ms-1s)



Siegel & Metzger 2017 PRL

tidal ejecta
shock-heated ejecta

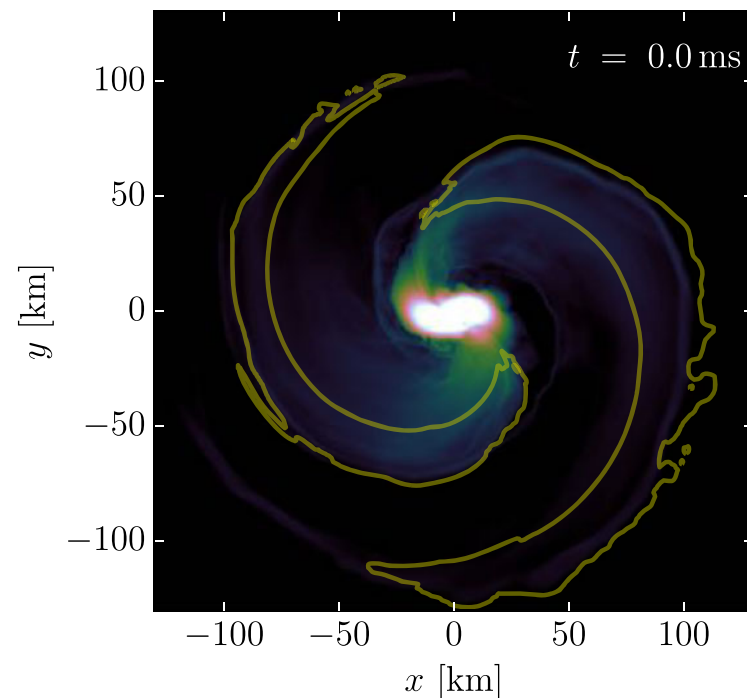
neutrino- and magnetically
driven wind

(binary NS mergers only!)

disk outflows

Dynamical ejecta (\sim ms)

tidal ejecta



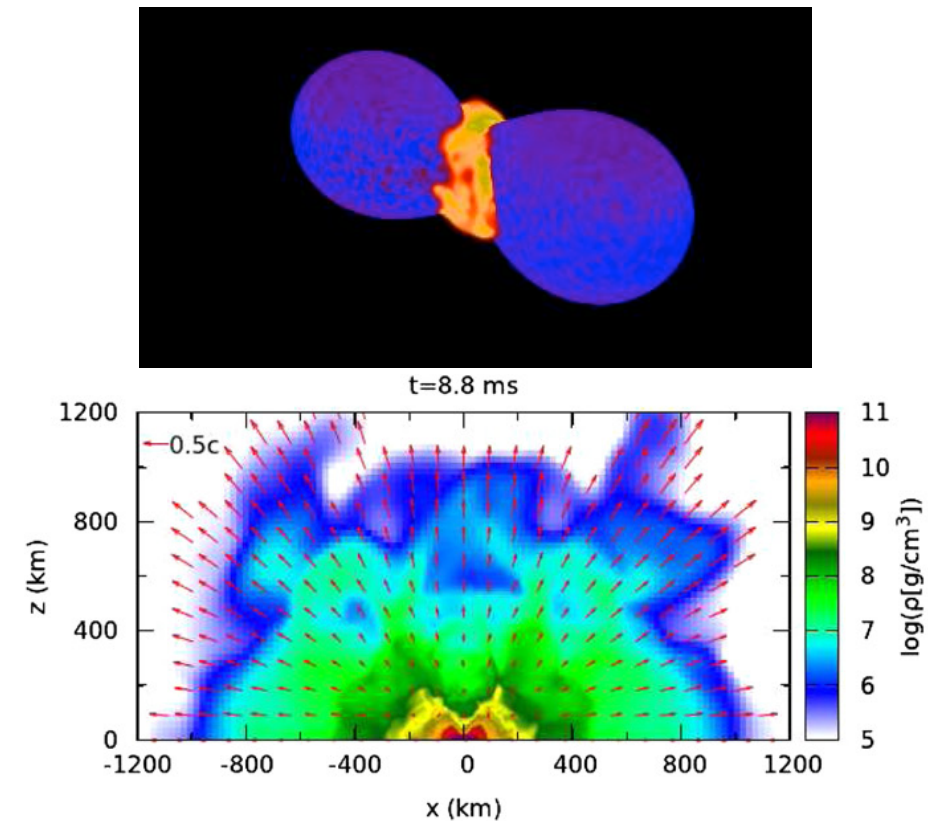
Ciolfi, Siegel+ 2017

- tidally ejected prior/at merger (leaking out of Lagrange points)
- fast: $v \sim 0.2c$
- cold, neutron-rich material from (' $T \sim 0$ K', $s < 10$ k_B, $Y_e < 0.1$)



fast red kilonova transient

shock-heated ejecta



Hotokezaka+ 2013, Bauswein+ 2013

- squeezed out from the shock interface at merger
- fast: $v > 0.2c$
- shock-heated \rightarrow hot: $T \sim 10$ MeV
- strong neutrino emission raises Y_e ($Y_e > 0.25$)

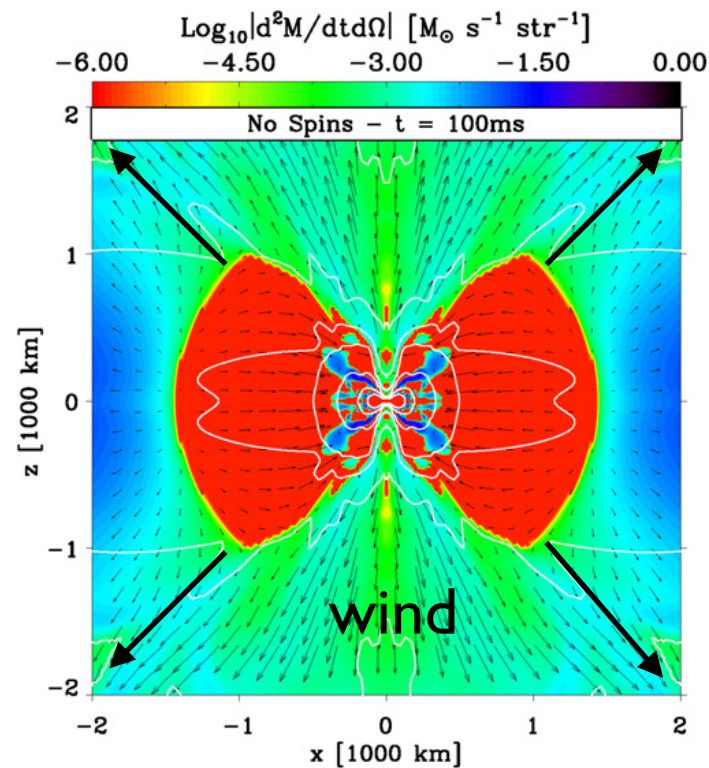


fast blue kilonova transient

$$M_{\text{tot}} \lesssim 10^{-3} M_{\odot}$$

Winds from remnant (metastable) NS

neutrino-driven winds



Dessart+ 2009

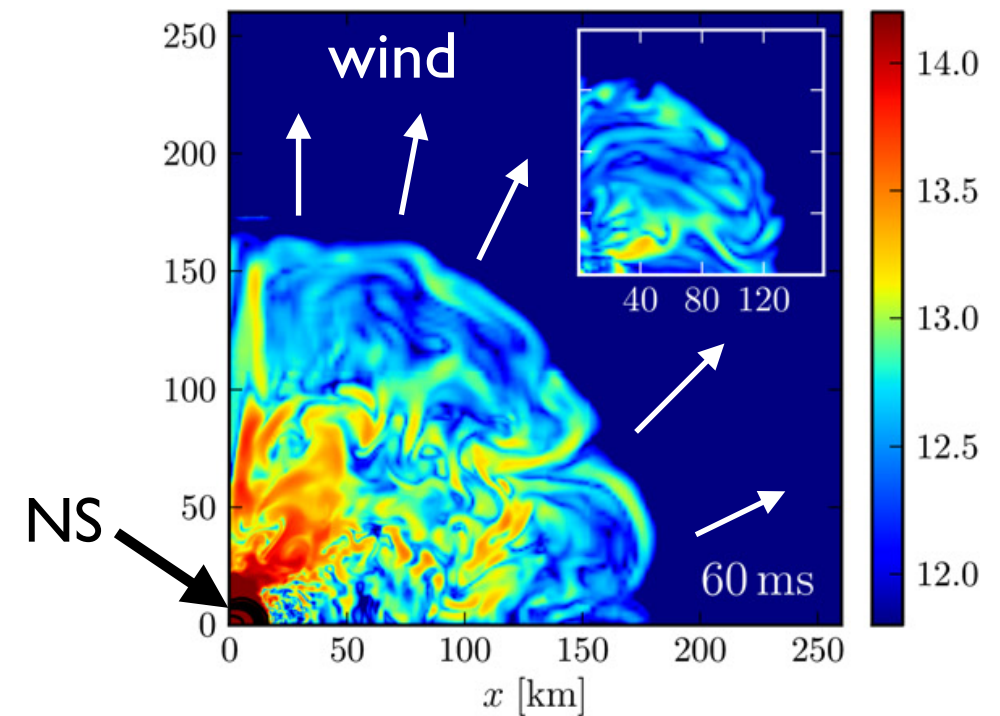
- **reabsorption of neutrinos** drives wind off the surface (similar to “gain layer” in core-collapse SNe)
- slow: $v < \sim 0.1c$
- hot: $T \sim 10$ MeV
- $Y_e > 0.25$ (due to reabsorption of neutrinos)
- $\dot{M}_{\text{in}} \sim (10^{-4} - 10^{-3}) M_{\odot} \text{s}^{-1}$



slow blue kilonova transient

(in certain regime both mechanisms can act together and generate **massive fast** ejecta) Metzger+ 2018

magnetically driven winds



Siegel+ 2014 Cioffi, Siegel+ 2017

- **magnetic field amplification** in stellar interior generates enhanced magnetic pressure that drives a wind from the surface layers (toroidal field gradients)
- slow: $v < \sim 0.1c$
- hot: $T \sim 10$ MeV
- $Y_e > 0.25$ (due to neutrinos irradiation)
- $\dot{M}_{\text{in}} \sim (10^{-3} - 10^{-2}) M_{\odot} \text{s}^{-1}$

Dynamical ejecta and winds

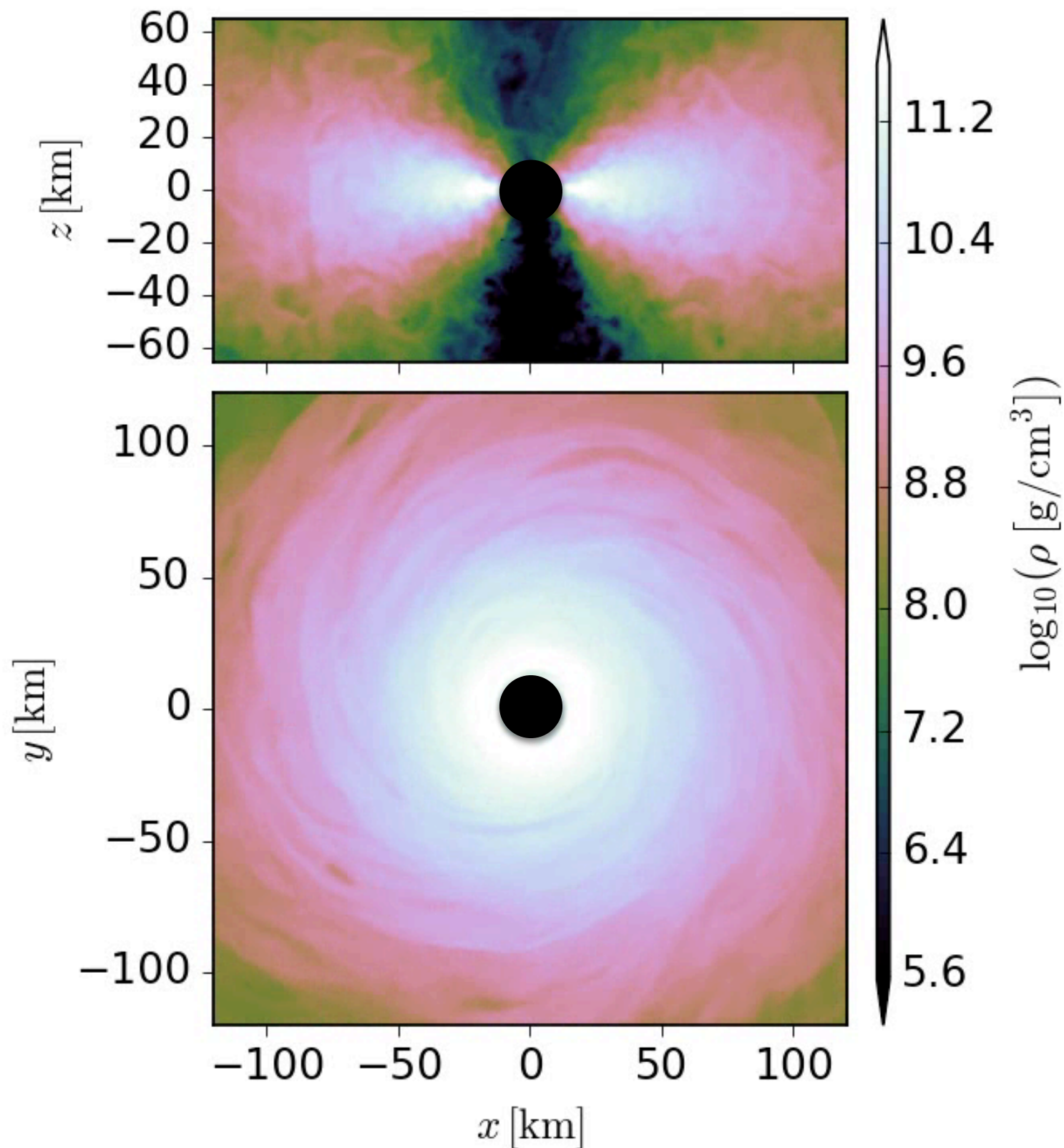


Movie: BNS merger showing dynamical ejecta and winds from remnant NS

Cioffi, Siegel+ 2017

Post-merger accretion disk outflows

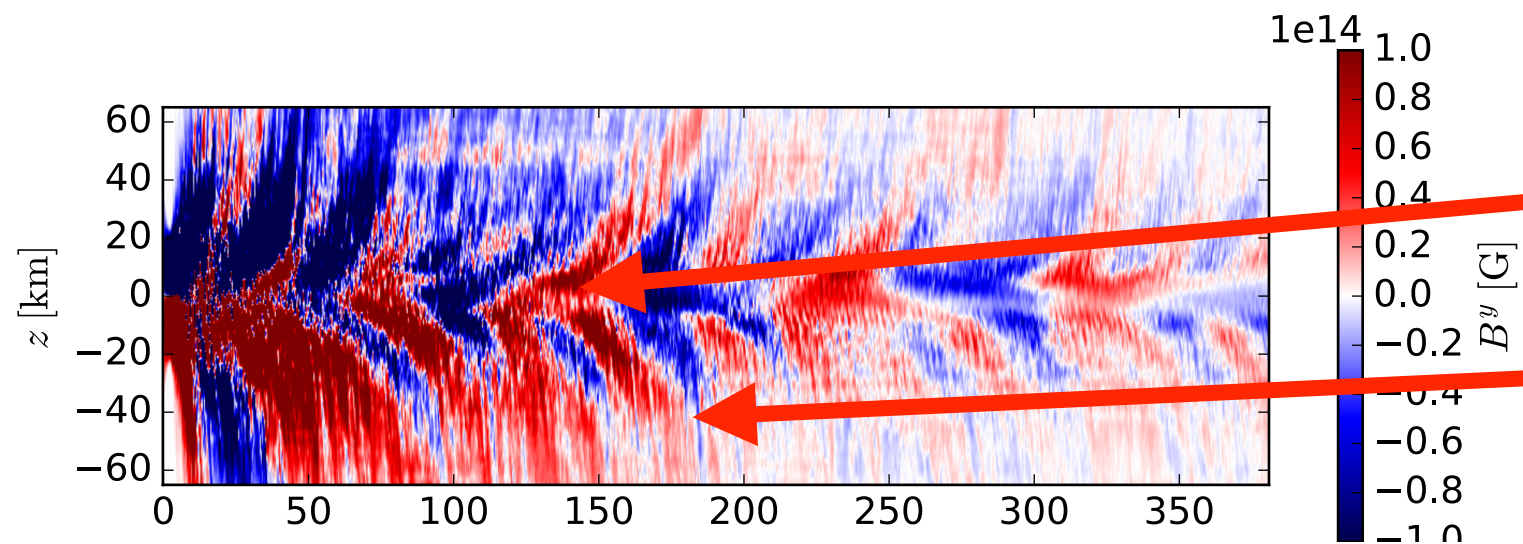
Siegel & Metzger 2017, PRL Siegel & Metzger 2018a



- imbalance of viscous heating from MHD turbulence and neutrino cooling off the disk midplane leads to formation of hot corona that launches thermal winds, further acceleration by seed particle formation

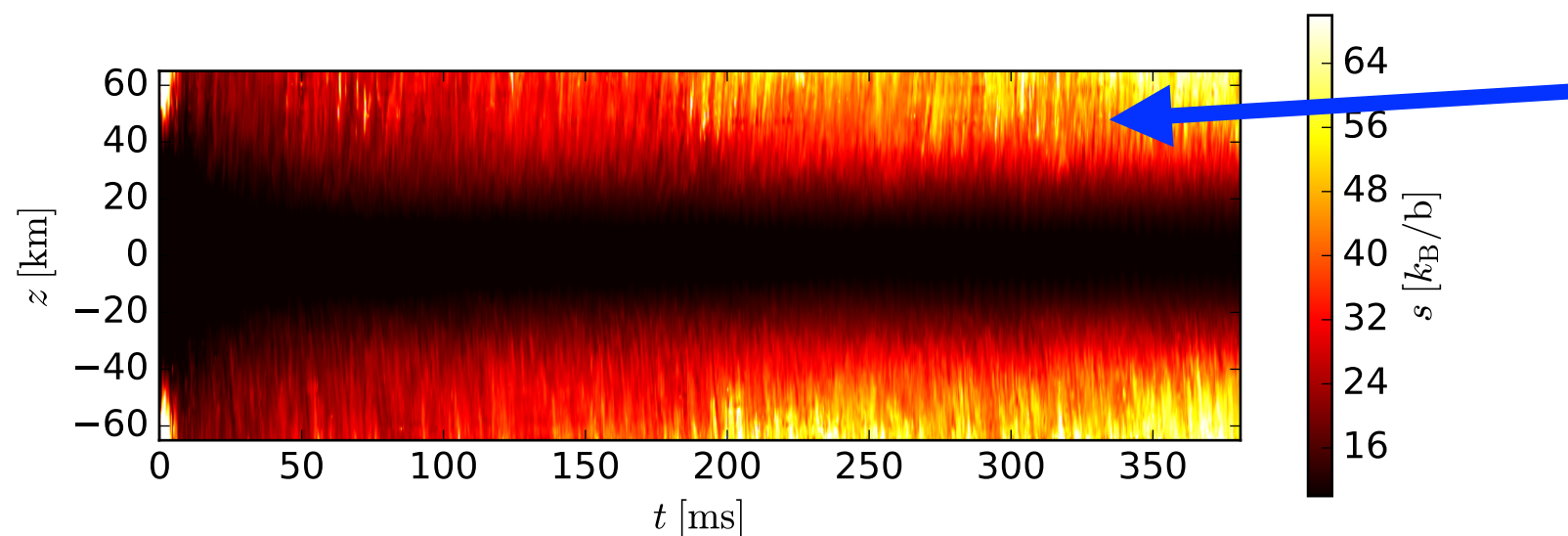
$t = 20.113 \text{ ms}$

Accretion disk dynamo & generation of outflows



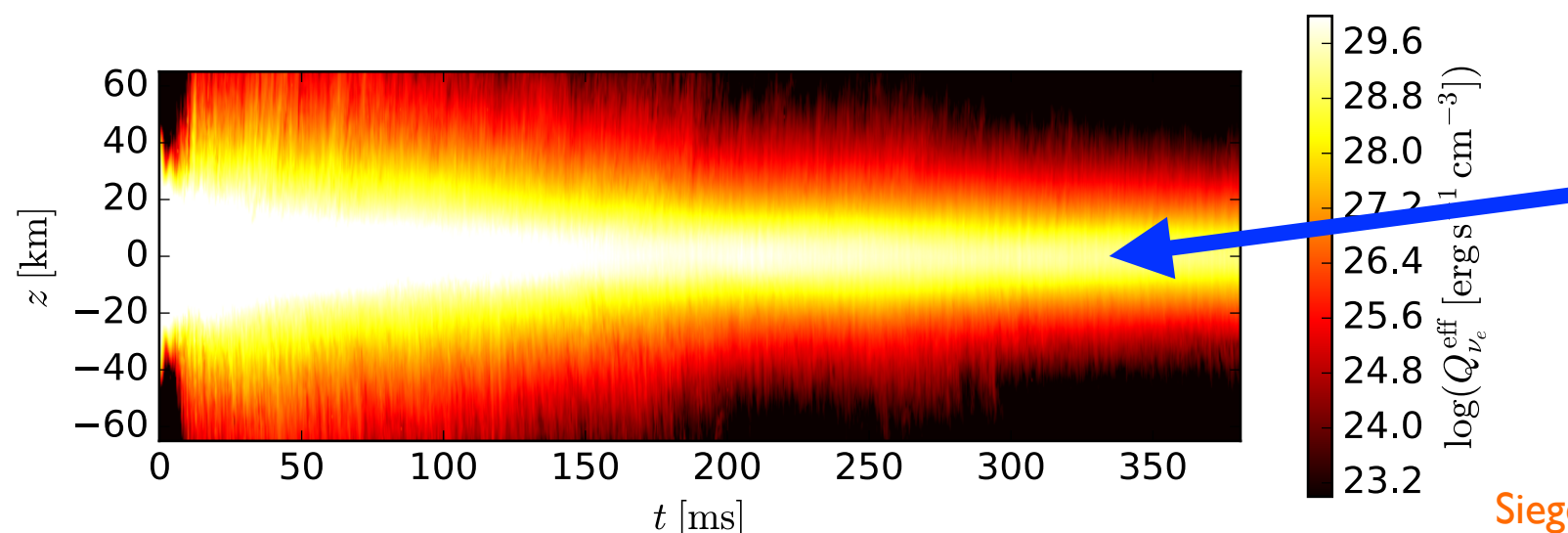
magnetic energy is generated in the mid-plane

- migrates to higher latitudes
- dissipates into heat off the mid-plane



→ “hot corona”

hot corona launches
thermal outflows
(neutron-rich wind)

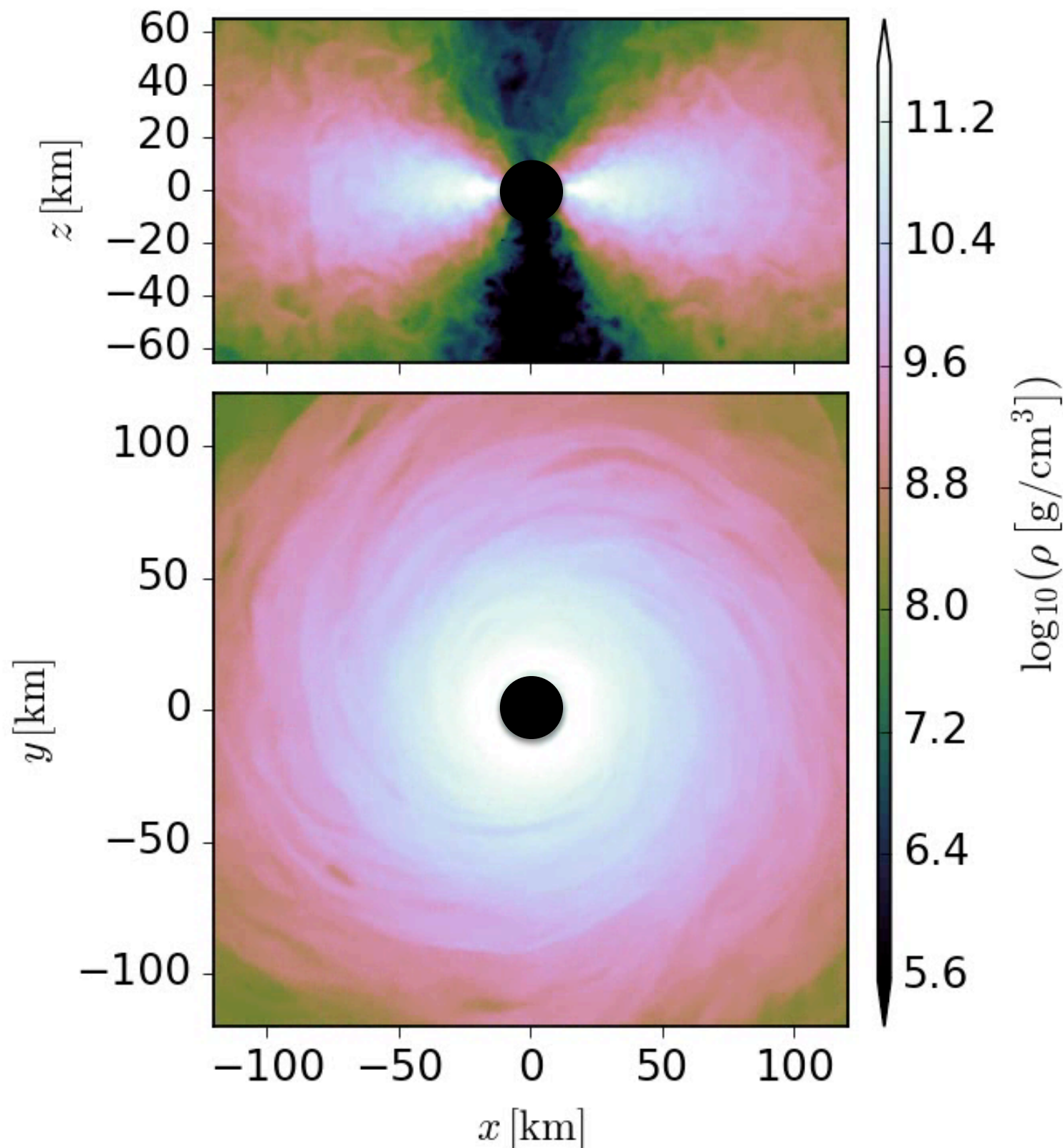


NS post-merger accretion disk are cooled from the mid-plane by neutrinos (rather than from the EM photosphere)!

Siegel & Metzger 2018

Post-merger accretion disk outflows

Siegel & Metzger 2017, PRL Siegel & Metzger 2018a



- imbalance of viscous heating from MHD turbulence and neutrino cooling off the disk midplane leads to formation of hot corona that launches thermal winds, further acceleration by seed particle formation
- slow: $v \sim 0.1c$
- hot: $T \sim 10 \text{ MeV}$
- $Y_e < 0.25$ if central object is a BH (due to self-regulation mechanism; details see ICTP colloquium)
- massive outflows (may dominate mass ejection in binary NS mergers):

$$M_{\text{tot}} \gtrsim 0.3 - 0.4 M_{\text{disk}}$$

$$\rightarrow \gtrsim 10^{-2} M_{\odot} \quad \text{cf. also: Fernandez+ 2018}$$



slow red kilonova (BH)

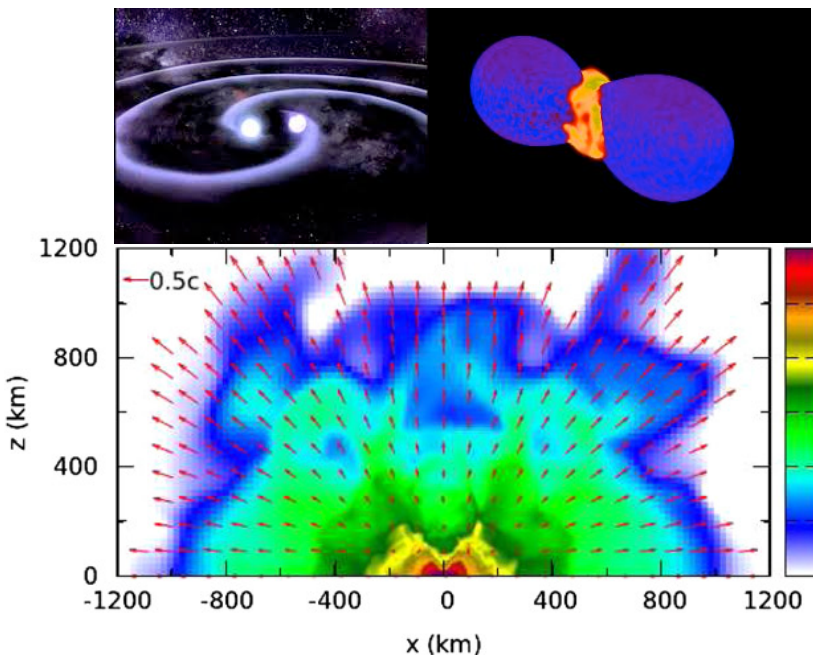
slow blue kilonova (long-lived remnant)

Lippuner+ 2017

$t = 20.113 \text{ ms}$

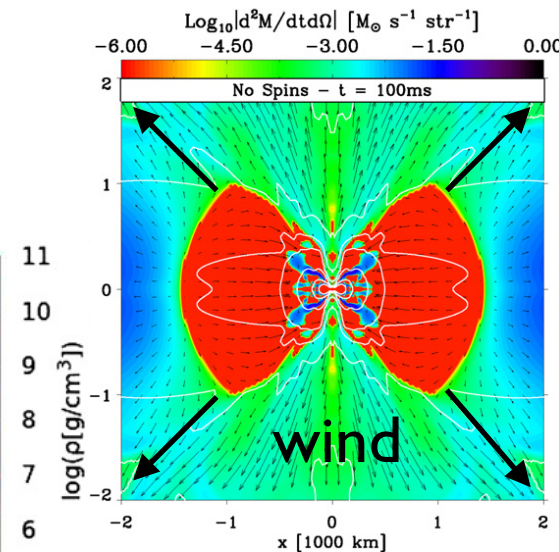
Sources of ejecta in NS mergers

dynamical ejecta (\sim ms)

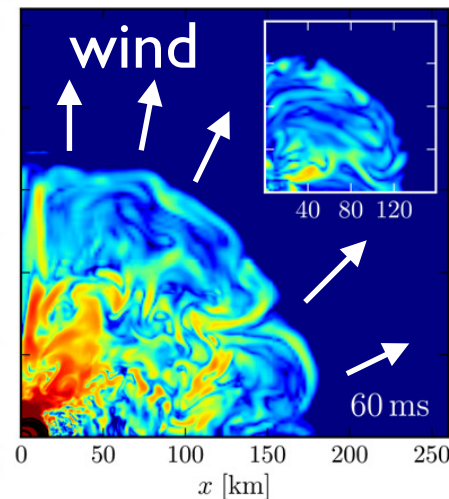


Hotokezaka+ 2013, Bauswein+ 2013

winds from NS remnant (\sim 10ms-1s)

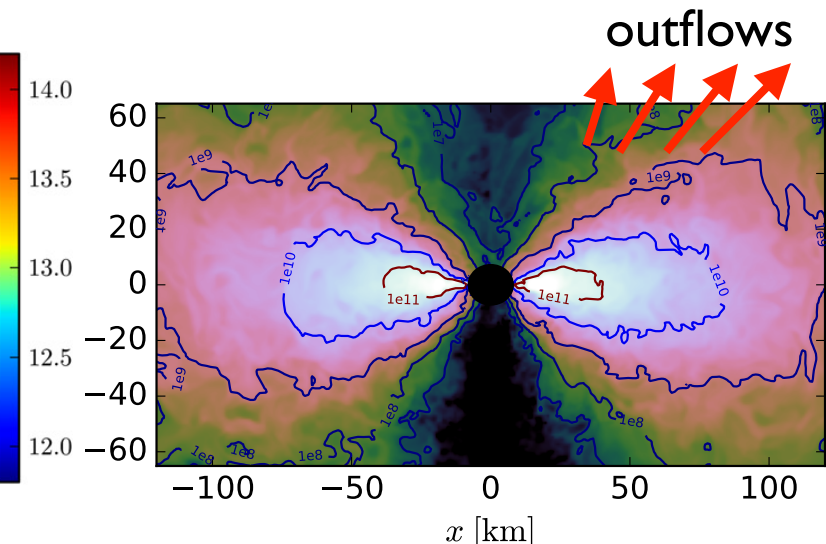


Dessart+ 2009



Siegel+ 2014
Ciolfi, Siegel+ 2017

accretion disk (\sim 10ms-1s)



Siegel & Metzger 2017, 2018

tidal ejecta
shock-heated ejecta

$$M_{\text{tot}} \lesssim 10^{-3} M_{\odot}$$

$$v \gtrsim 0.2c$$

neutrino-driven wind

$$\dot{M}_{\text{in}} \sim (10^{-4} - 10^{-3}) M_{\odot} \text{s}^{-1}$$

magnetically driven wind

$$\dot{M}_{\text{in}} \sim (10^{-3} - 10^{-2}) M_{\odot} \text{s}^{-1}$$

thermal outflows

$$M_{\text{tot}} \gtrsim 0.3 - 0.4 M_{\text{disk}}$$

$$v \sim 0.1c$$

Overall ejecta mass per event:

$$\lesssim 10^{-3} - 10^{-2} M_{\odot}$$

strongly depends on EOS and mass ratio

Bauswein+ 2013
Radice+ 2016, 2017
Sekiguchi+ 2016
Palenzuela+2015
Lehner+2016
Ciolfi, Siegel+2017

Siegel & Metzger 2017, 2018

$$\gtrsim 10^{-2} M_{\odot}$$

lower limit